Chapter 18

Fourier Transform Resonators

18.1 Self-Filtering Unstable Resonators

As was discussed in Sec.7.2.2, unstable resonators exhibit a considerable amount of power in the side lobes of the far field, especially if the magnification is low. One way to decrease the power fraction in the side lobes is the utilization of variable reflectivity mirrors as output couplers, as seen in Sec. 7.7. A different approach to enhance the shape of the far field intensity distribution is the spatial filtering of the electric field inside the resonator. If the resonator exhibits an intracavity focus point at a certain plane, this plane is conjugate to the focal plane generated by the focusing optics outside the resonator. The insertion of a spatial filter (e.g. an aperture or a filter with a defined lateral transmission profile) at the intracavity focal plane will, therefore, generate the same intensity distribution at the extracavity focal plane. In general, the field distribution at the intracavity focal plane is the Fourier transform of the field at the resonator mirrors. This type of resonator, therefore, is referred to as the Fourier transform resonator or self-filtering resonator [5.22-5.26,5.31,5.32]. The schematic of a self-filtering unstable resonator (SFUR) is shown in Fig. 18.1. The resonator is confocal which means that both mirrors generate a focal spot at the same plane. The basic principle of this resonator is the transformation of a rectangular intensity profile into a Gaussian one by cutting off the side lobes of the Fourier transform with an aperture.

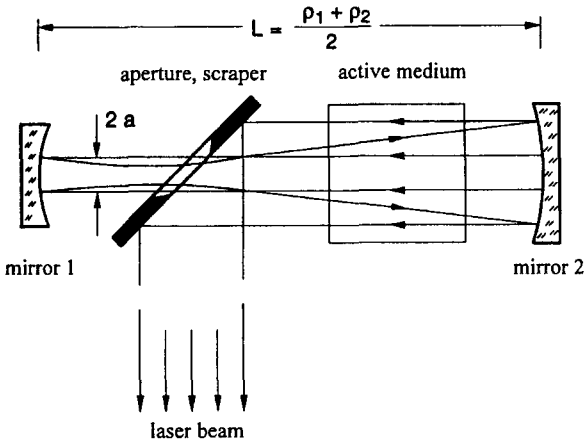

Fig. 18.1 Negative branch confocal unstable resonator with self-filtering. The aperture shapes the intensity profile by filtering the Fourier transform and serves as an output coupler at the same time (ρ_i: radius of curvature of mirror *i*).

The electric field incident on the aperture from the right mirror generates its Fourier transform at the aperture after being reflected by mirror 1 (Fig. 18.2). If we assume that the intensity distribution of the field traveling towards mirror 1 exhibits a flat-top profile behind the aperture, the intensity distribution at the aperture is determined by the Fourier transform of a circular aperture with radius a. The first minimum of this intensity distribution is located at the radius:

$$r_0 = 0.61 \frac{\lambda}{a} \frac{\rho_1}{2} \tag{18.1}$$

where λ is the wavelength of the electric field and ρ_1 is the radius of curvature of mirror 1. The aperture radius a is chosen equal to r_0 to cut off the side lobes of the Fourier transform:

$$a = \sqrt{0.305 \lambda \rho_1} \tag{18.2}$$

The truncation of the Fourier transform generates an intensity profile that can be approximated by a Gaussian beam with a beam waist radius of:

$$w_{B1} = 0.43 \frac{\lambda}{a} \frac{\rho_1}{2} \tag{18.3}$$

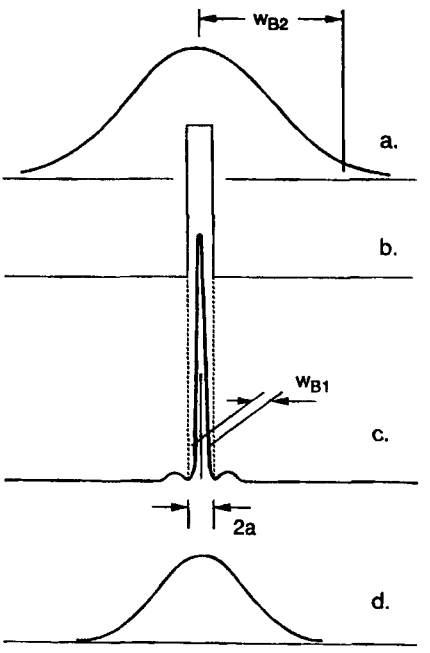

Fig. 18.2 Radial intensity distributions inside a self-filtering unstable resonator (SFUR). a) at the aperture, incident from mirror 2, b) behind the aperture, incident from mirror 2, c) at the aperture, incident from mirror 1, and d) at mirror 2.

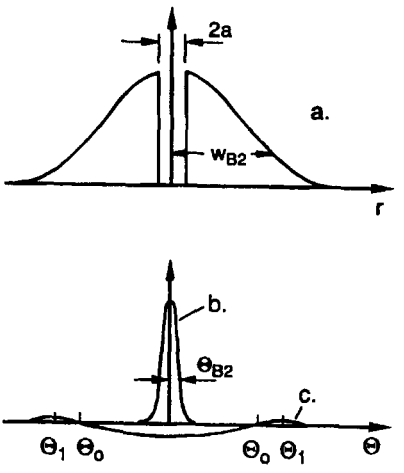

Fig. 18.3 Radial field distributions in the near field and the far field of a self-filtering unstable resonator (SFUR). a) at the aperture, b) far field of the Gaussian profile, c) far field of the circular aperture.

After reflection from mirror 2, the beam radius of the Gaussian intensity distribution at the aperture is given by:

$$w_{B2} = \frac{a}{0.43\ \pi}\ \frac{\rho_2}{\rho_1} = 0.74\ M\ a \tag{18.4}$$

where $M = \rho_2/\rho_1$ is the magnification of the confocal unstable resonator. Unfortunately, the approximation of the truncated Airy pattern by a Gaussian profile is too rough. Since the Airy pattern exhibits steeper slopes, it is to be expected that the beam radius at the aperture is larger than predicted by (18.4). A more accurate treatment of the beam propagation, in fact, shows that the magnified intensity distribution at the scraper can be described by a Gaussian profile with a beam radius of [5.28]:

$$w_{B2} = 0.974\ M\ a \tag{18.5}$$

The near field intensity distribution is thus given by a Gaussian beam profile with the center core of radius a missing. The diffraction at the aperture generates small side lobes in the far field. The far field amplitude distribution $E(\theta)$ can be calculated by subtracting the far field of a circular aperture with radius a from the far field of the Gaussian beam (Fig. 18.3). With the assumption that $w_{B2} \gg a$, the final result reads:

$$E(\theta) = C\left(\exp\left[-\frac{\theta\pi w_{B2}}{\lambda}\right] - \left[\frac{a}{w_{B2}}\right]^2 \frac{J_1(2\pi\theta a/\lambda)}{\pi a\theta/\lambda}\right) \tag{18.6}$$

where J_1 is the Bessel function of order 1 and θ is the angle of divergence. Compared to a conventional unstable resonator with the same magnification M, the self-filtering decreases the side lobes considerably (Fig. 18.4). However, this improvement of the beam quality is a result of an increase in the diffraction losses. The loss factor V (=1-loss) of the SFUR due to output coupling can be calculated assuming a Gaussian intensity profile with the beam radius w_{B2} given by (18.5). For $a \ll w_{B2}$, we get:

$$V = \frac{\pi a^2}{0.5 \pi w_{B2}^2} = \frac{2.108}{M^2} \tag{18.7}$$

In addition to the output coupling loss, the truncation of the Airy pattern results in an additional loss of 16% per round trip. Thus, the total loss factor per round trip of the SFUR is given by:

$$V_{tot} = 0.84 V = \frac{1.771}{M^2} \tag{18.8}$$

A comparison of the far field properties of conventional and self-filtering unstable resonators indicates that at the same round trip loss, both resonators provide a similar power content in the side lobes (Fig. 18.4). For conventional unstable resonators with equivalent Fresnel numbers N_{eq} around 0.5, the round trip loss factor is higher than the one for the SFUR given by (18.8). Therefore, the conventional unstable resonators can be operated at a higher magnification $M^* > M$, resulting in near field and far field distributions similar to those of a SFUR with magnification M. This leads us to the conclusion that the SFUR is not superior to a conventional unstable resonator as far as the beam quality is concerned. Furthermore, the loss generated by the truncation of the Fourier transform may considerably decrease the output power if a low gain medium is used. However, for lasers that emit at small wavelengths (like in excimer lasers), the design of conventional unstable resonators with equivalent Fresnel numbers on the order of 0.5 would lead to a small diameter of the high reflecting spot on the output coupling mirror (on the order of 0.5mm). High peak powers might damage the output coupler and it is, therefore, safer to use a scraper at an angle of 45° to couple out the beam. Placing the scraper at the focal plane is just a convenient way to realize the output coupling. SFURs have been successfully implemented in excimer, CO_2, and Nd:YAG lasers [5.27-5.34]. In addition to the Gaussian intensity distribution in the near field, a second advantageous property of the SFUR is the high discrimination against higher order transverse modes. This results in a fast establishment of the steady-state fundamental mode, a feature that is of crucial importance for active media with a very short population inversion lifetime. However, the disadvantage of the SFUR is the dependence of the mode volume on the wavelength. Combination of (18.2) and (18.5) yields for the cross sectional area of the beam in the active medium:

$$A_b = \pi w_{B2}^2 = 0.91 M^2 \lambda \rho_1 \tag{18.9}$$

At short wavelengths, where the SFUR is of particular interest, it is not possible to fill a large diameter active medium without choosing a long resonator (Fig. 18.5). However, shorter resonator set-ups can be realized with nonconfocal SFURs [5.31].

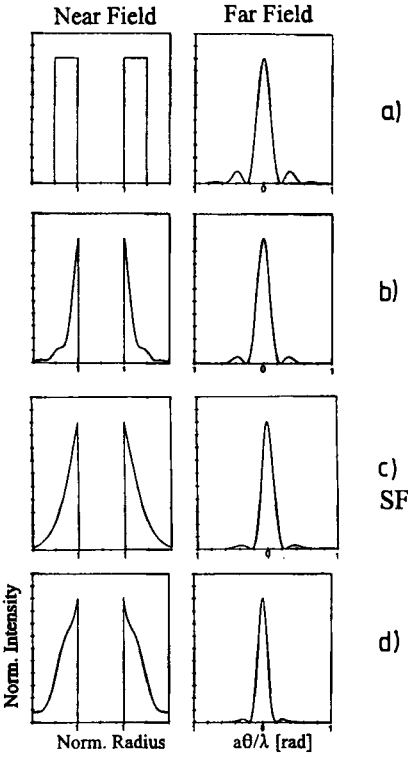

Fig. 18.4 Comparison of the radial intensity distribution in the near field and the far field of unstable resonators with magnification $M=2$. a) conventional unstable, geometric, loss factor =0.25, b) conventional unstable, with diffraction and $N_{eq}=0.5$, loss factor =0.55, c) SFUR, loss factor=0.44. Figure d) presents the far field for a conventional unstable resonator with $M=2.5$ and $Neq=0.5$, which means that this resonator exhibits a total loss similar to that of the SFUR in c).

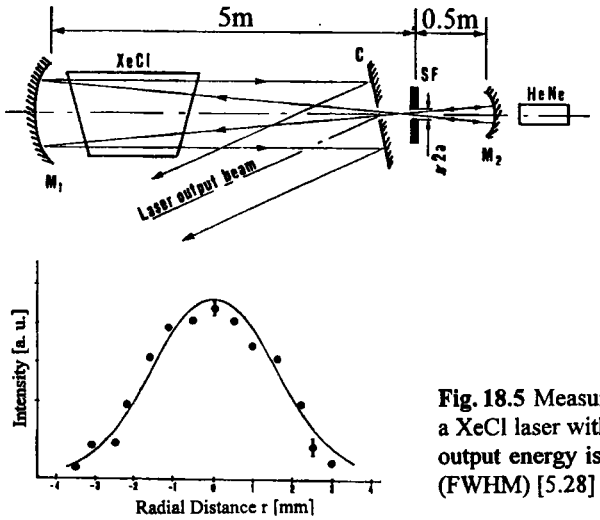

Fig. 18.5 Measured near field intensity distribution of a XeCl laser with SFUR ($\lambda=308nm$, $a=0.3mm$). The output energy is 120mJ at a pulse duration of 90ns (FWHM) [5.28] (© IEEE 1987).

18.2 Stable Fourier Transform Resonators

The concept of self-filtering can also be applied to stable resonators. In contrast to the SFUR, the spatial filter is only used to put a constraint on the Fourier transform and output coupling is accomplished by means of a conventional partially reflecting mirror. The design of a stable Fourier transform resonator is determined by the fact that the field at the active medium or at the output coupling mirror is the Fourier transform of the field at the spatial filter. Therefore, we need appropriate intracavity transformation optics that provide a Fourier transformation between two planes. In general, such transformation optics are described by a ray transfer matrix of the following form:

$$M_{FT} = \begin{pmatrix} 0 & B \\ C & 0 \end{pmatrix} \tag{18.10}$$

The two simplest optical systems that provide an optical Fourier transformation between the input and the output plane are depicted in Fig. 18.6. Based on these two set-ups we can design Fourier transform resonators by placing the spatial filter at the input plane and the active medium at the output plane. The two resonator mirrors have to be added in such a manner that the fields at both planes represent self-consistent solutions for a resonator round trip. With design b), the use of flat mirrors at both the input and output plane results in a resonator that is equivalent to a confocal resonator ($g_1=g_2=0$) (Fig.18.7a). A true confocal resonator is obtained with design a) by replacing the two lenses with resonator mirrors that provide the same imaging properties ($\rho=f$) which means that the mirror distance is equal to the curvature of both mirrors (Fig. 18.7b). We already discussed the Fourier transform properties of the confocal resonator in Sec. 6.3 using circular apertures as spatial filters.

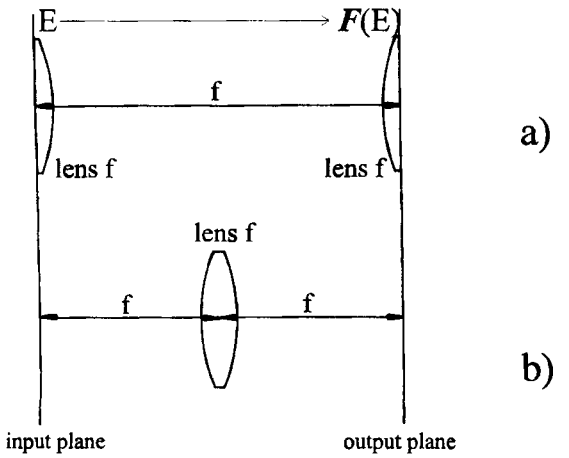

Fig. 18.6 Optical systems that provide the Fourier transform $F(E)$ of the input field E at the output plane.

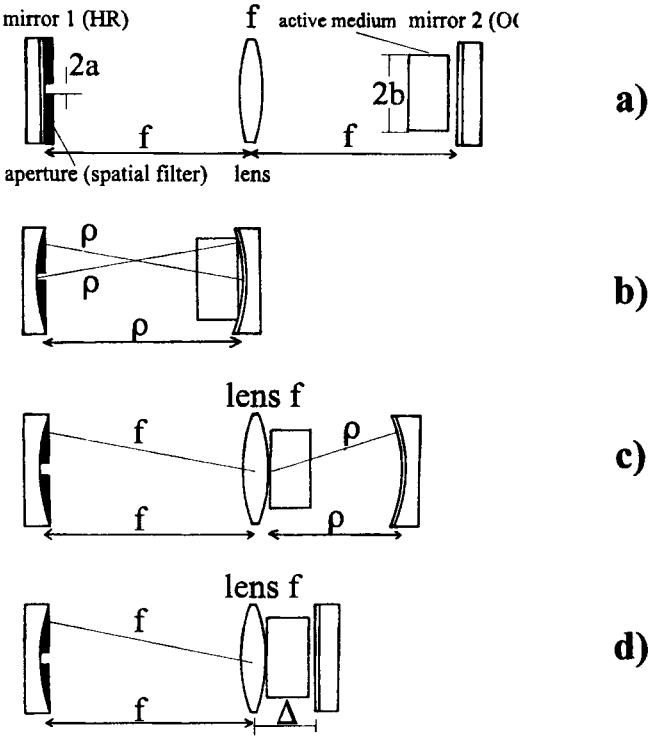

Fig. 18.7 Stable Fourier transform resonators. a) equivalent confocal ($g_1=g_2=0$), b) confocal ($g_1=g_2=0$), c) concentric ($g_1g_2=1$ and $g_1<0$), d) vanishing g-parameter of mirror 1 ($g_1=0$).

Whereas in Fig. 18.7a) and b) the fields on the two resonator mirrors are related to each other via a Fourier transform, the resonator in Fig. 18.7c) generates the Fourier transform of the field at the aperture at the left face of the active medium. The curvature of the right mirror is chosen so that this plane is imaged onto itself. The equivalent g-parameters of this resonator are given by:

$$g_1 = -\frac{\rho}{f} \quad , \quad g_2 = -\frac{f}{\rho} \tag{18.11}$$

Thus the resonator is concentric. The resonator in Fig. 18.7d) does not exactly reproduce the field distribution at the left face of the active medium. However, this Fourier transform resonator will also work provided that the Fresnel number of the right resonator segment $b^2/(2\Delta\lambda)$is high enough (greater than 30). In this case the propagation of the field to the right mirror and back can be described by geometric optics since the spread of the field due to diffraction is negligible.

All four resonators are equivalent as far as the Fourier transformation and the optimization of the resonator set-up are concerned. If we assume that the spatial filter supports a Gaussian beam with a beam radius w_1 at mirror 1, the beam radius in the active medium is given by:

$$w_2 = f\,\theta = \frac{f\,\lambda}{\pi\, w_1} \tag{18.12}$$

where θ is the half angle of divergence of the Gaussian beam. For the confocal resonator in Fig. 18.7b), the focal length f has to be replaced by the mirror curvature ρ in (18.12) and all equations derived below. Let us first make the assumption that we can use a circular aperture to generate the Gaussian beam (which means that diffraction losses at the aperture are negligible). We saw in Chapter 11.2 that the maximum output power in fundamental mode operation is attained if the radii of intracavity apertures are about 1.3 times larger than the Gaussian beam radii. Equation. (18.12), therefore, can be written as:

$$\frac{a\,b}{f\,\lambda} = \frac{(1.3)^2}{\pi} \approx 0.54 \tag{18.13}$$

where a is the aperture radius and b is the radius of the active medium. This gives us a first idea of how to choose the aperture dimensions to attain a near diffraction limited beam. An exact treatment of the field propagation using diffraction integrals reveals that the intensity distribution of the fundamental mode is in fact almost Gaussian, and optimum performance in fundamental mode operation is obtained for [5.36]:

$$\frac{a\,b}{f\,\lambda} \approx 0.6 \tag{18.14}$$

Unfortunately, the Gaussian beam only provides a fill factor in the active medium of less than 0.9, which means that at least 10% of the available power cannot be extracted. In order to realize a fill factor close to 1.0 it is necessary to generate a flat-top intensity profile with radius b at the active medium (with a planar wave front). In order to generate this homogeneous filling of the active medium, the radial field distribution at mirror 1 must be the Airy pattern (see Sec. 2.2.2):

$$E(r) = \frac{2\pi b^2}{\lambda f}\, E_0\, \frac{J_1[2\pi rb/(\lambda f)]}{2\pi rb/(\lambda f)} \tag{18.15}$$

where E_0 is the electric field amplitude at the active medium and r is the radial coordinate at mirror 1.

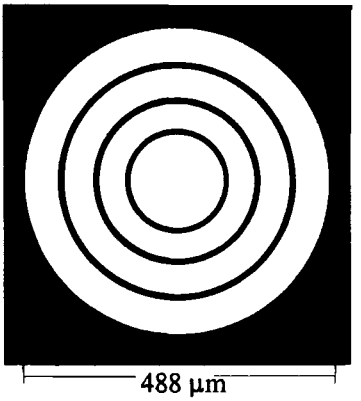

Fig. 18.8 A spatial filter which supports the Airy pattern in a Fourier transform resonator (λ=*1μm*, *f=300mm*, *b=3mm*). The black areas absorb the electric field, the white areas exhibit 100% transmission. This filter is placed in front of the high reflecting mirror 1.

To a good approximation, the Airy pattern exhibits zero intensity at the radii:

$$r_m = m\ 0.61\ \frac{f\lambda}{b}, \qquad m = 1,2,3,... \tag{18.16}$$

An appropriate spatial filter to generate a flat-top beam profile in the active medium, therefore, should absorb or deflect the electric field in the vicinity of the zero intensity lines of the Airy pattern. In practice, it is sufficient to take only the first couple of rings into consideration (Fig. 18.8). The widths of the rings have to be optimized to efficiently discriminate against unwanted transverse modes without generating losses that are to high for the fundamental mode. Such a spatial filter can be produced via photoedging using a focused laser beam with a flat-top near field beam profile. This technique was successfully applied in [5.37] to generate a diffraction limited output beam in a Q-switch Nd:YAG laser using a confocal resonator (Fig. 18.9). Other examples of stable Fourier transform resonators can be found in [5.38-5.40].

The reader should keep in mind that stable Fourier transform resonators are extremely sensitive to variations in the distances between the optical elements. This is the result of their location on the stability limits in the g-diagram. As was presented in Sec. 6.3 for the confocal resonator, a tight length tolerance of less than ±0.5% must be maintained to prevent a decrease of output power by more than 10%. If the active medium exhibits thermal lensing, the corresponding refractive power has to be compensated by the resonator design. Therefore, a similarly tight tolerance has to be kept on the pump power going into the active medium which means that the output power cannot be varied. Furthermore, the gain saturation inside the active medium will modify the mode structure. For the confocal Fourier transform resonators (Fig. 18.7a,b), the field distribution at mirror 2 is not the exact Fourier transform of the field distribution at the spatial filter. The losses generated by the filter, therefore, will slightly rise as the small-signal gain of the active medium is increased.

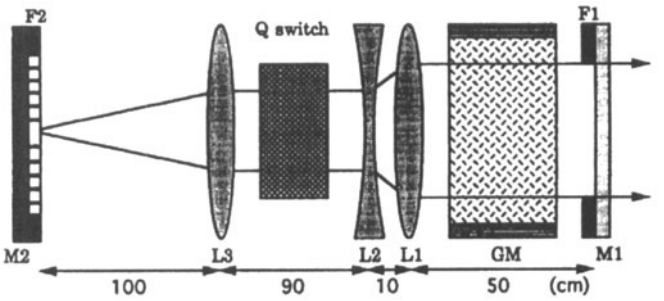

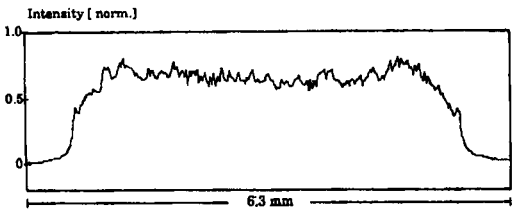

a)

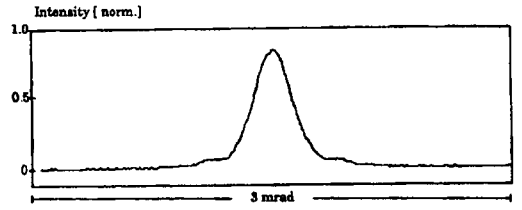

b)

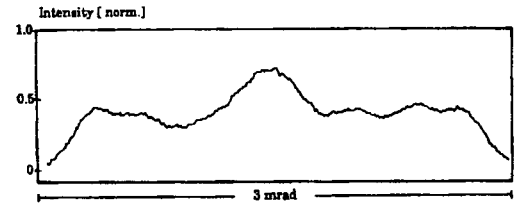

c)

Fig. 18.9. Measured radial intensity profiles in the near field a) and in the far field b) of a Nd:YAG Q-switch laser (λ=1.064μm) with a confocal Fourier transform resonator. (rod diameter: 0.25", focal lengths: L_1=*12.5cm*, L_2=*-5cm*, L_3=*100cm*). The spatial filter consists of eleven rings of 80μm width that correspond to the nodal lines of the Airy pattern. The output energy per pulse is 200mJ at a pulse duration of 60ns and a repetition rate of 10Hz (electrical input energy per pulse: 25J, pump pulse duration: 200μs). The repetition rate could be varied between 5Hz and 10Hz with minor variations in the distance between the lenses L_1 and L_2. Without the spatial filter an output energy of 210mJ and a full angle of divergence of about 3mrad was measured (Fig. c) [5.37] (© OSA 1993).